REVIEW

How Enzymes Work: Analysis by Modern Rate Theory and Computer Simulations

Mireia Garcia-Viloca,[1] Jiali Gao,[1] Martin Karplus,[2]* Donald G. Truhlar[1]*

Advances in transition state theory and computer simulations are providing new insights into the sources of enzyme catalysis. Both lowering of the activation free energy and changes in the generalized transmission coefficient (recrossing of the transition state, tunneling, and nonequilibrium contributions) can play a role. A framework for understanding these effects is presented, and the contributions of the different factors, as illustrated by specific enzymes, are identified and quantified by computer simulations. The resulting understanding of enzyme catalysis is used to comment on alternative proposals of how enzymes work.

Enzyme catalysis, which can produce rate accelerations as large as a factor of 10^{19} (*1*), involves molecular recognition at the highest level of development. The catalysis of many proton-transfer reactions, for example, requires the recognition of a change in a CH bond length of about 0.5 Å in going from the reactant to the transition state. In 1946, before structural information was available, Linus Pauling proposed (*2*) that enzymes can accelerate rates because they bind the transition state better than the substrate and thereby lower the activation energy. This key concept in enzyme catalysis can now be augmented by a detailed description of the sources of enzymatic rate enhancements based on developments in transition state theory, the availability of structural, kinetic, and thermodynamic data, and the insights provided by computer simulations. An overview of our present understanding of enzyme catalysis is particularly timely because of the increasing number of articles that propose a variety of origins for enzyme catalysis; these are described by terms such as correlated conformational fluctuations, dynamical and nonequilibrium effects, electrostatic pre-organization, entropic guidance, fluctuating barrier height, near-attack configurations, reactant destabilization, and tunneling. We show that these proposals all fit into the framework that we develop and that their role in enzyme catalysis, whether large or small, can be understood in terms of this framework.

[1]Department of Chemistry and Supercomputing Institute, University of Minnesota, Minneapolis, MN 55455, USA. [2]Department of Chemistry and Chemical Biology, Harvard University, Cambridge, MA 02138, USA, and Laboratoire de Chimie Biophysique ISIS, Université Louis Pasteur, 67000 Strasbourg, France.

*To whom correspondence should be addressed. E-mail: marci@tammy.harvard.edu, truhlar@umn.edu

In an insightful paper published in 1978 (*3*), which is as valid today as it was then, Schowen wrote, in accord with Pauling's original insight, "…the entire and sole source of catalytic power [of enzymes] is the stabilization of the transition state…" In the present review, we introduce modern concepts of transition state theory that led to a somewhat modified and more detailed description of the role of the transition state and use it as the framework for describing our present understanding of how enzymes "work." Our restatement of the key premise is that "the entire and sole source of the catalytic power of enzymes is due to the lowering of the free energy of activation and any increase in the generalized transmission coefficient, as compared to that of the uncatalyzed reaction." In what follows, we outline the aspects of transition state theory required for justifying this statement and then use the formulation in an analysis of the origin of the rate enhancements by enzymes (*4*); the examples considered are listed in Table 1.

Theoretical Background

Generalized transition state theory (*5*–*9*) provides a framework for understanding chemical reactions, whether they occur in the gas phase, in solution, or in enzymes. The rate constant for a reaction as a function of the temperature T takes the convenient form

$$k(T) = \gamma(T)(k_B T/h)(C^0)^{1-n} \exp[-\Delta G^{TS,0}(T)/RT] \quad (1a)$$

where C^0 is the standard state concentration, n is the order of the reaction, R is the gas constant, T is the temperature, and $\Delta G^{TS,0}$ is the standard-state quasithermodynamic free energy of activation (*10*), i.e., the difference between the standard-state molar free energy of the transition state and that of the reactants. The factor $(k_B T/h)$ is a frequency factor, equal to about 6 ps^{-1} at 300 K, for crossing the transition state and is valid in solution as well as in the gas phase (*11*); the generalized transmission coefficient, $\gamma(T)$, relates the actual rate for the reaction to that obtained from simple transition state theory, which has $\gamma(T)$ equal to unity. We note also that the choice of the reaction coordinate and the dividing surface are somewhat arbitrary and that the correct result for the rate constant $k(T)$ is obtained if $\Delta G^{TS,0}(T)$ and $\gamma(T)$ are calculated in a consistent manner (*7*, *12*).

A many-body system, such as a liquid or an enzyme in solution, can have a large number of reactive paths (*13*, *14*), each with one or more saddle points, so that the reaction dynamics is expected to be more complex than that found in small-molecule gas-phase reactions. For the latter, the potential surface often has a single valley leading to a single saddle point, and we sum over paths through that valley. In complex systems like enzymes we have to average over many reactant conformations and sum the rate over paths that proceed through many valleys, which can differ in conformational degrees of freedom, hydrogen bonding patterns, and so forth. However, this effect is automatically included in the transition state formalism because all reactive paths must pass through the dividing surface separating reactants from products.

The generalized transmission coefficient, $\gamma(T)$, can be expressed (*9*) as a product

$$\gamma(T) = \Gamma(T)\kappa(T)g(T) \quad (1b)$$

which makes explicit the three contributions. The first, $\Gamma(T)$, arises from dynamical recrossing. Thus, $\Gamma(T)$ is less than or equal to 1 because for any choice of transition state, some trajectories that cross it in the direction of products originate as products or recross the dividing surface to return to the reactant region (*15*). The second, $\kappa(T)$, arises from the contribution of quantum mechanical tunneling; therefore, almost always, $\kappa(T)$ is greater than or equal to 1. This correction is necessary because $\Delta G^{TS,0}$ includes only one of the major quantum effects, namely, quantization of the bound vibrations; the increase in the

Table 1. Enzymes mentioned in the discussion.

Enzyme*	Function	Mechanism
Acyl–CoA dehydrogenase (*72*) (FAD)	Catalyzes the oxidation of fatty acid thioesters conjugated to coenzyme A to yield *trans*-α,β-CoA product and $FADH_2$.	The oxidation of acyl-CoA substrate consists of an initial proton abstraction of the α-proton of the thioester by an Asp residue. The enolate ion intermediate is stabilized by hydrogen bonding interactions with a hydroxyl group of the FAD and a protein backbone amide group. The FAD cofactor is subsequently reduced through a hydride transfer from the β-carbon atom. Computational studies indicate that protein reorganization along the reaction path plays an important role in the enzyme.
Chorismate mutase (*33*, *37*, *60–65*)	Catalyzes the conversion of chorismate to prephenate, which is an intramolecular Claisen rearrangement.	The enzyme binds and stabilizes the reactive pseudo-diaxial conformation of chorismate, which is unstable in water. The more polar transition state is further stabilized by electrostatic interactions.
Corrinoid mutase (*77–79*) (AdoCBl)	Catalyzes 1,2 rearrangements (interchange of a hydrogen atom and a variable group between adjacent carbon atoms).	The highly reactive free radical species is generated by homolytic cleavage of a C-Co bond that is weakened by steric repulsion due to a protein-conformation change induced by substrate binding.
Cycloartenol synthase (*35*)	Catalyzes cationic cyclization of oxidosqualene.	In all terpenoid cyclases, the folding of the substrate upon binding in the active site dictates the carbocation cyclization product; steric effects are the key to the control of regio- and stereoselectivity. In the well-studied oxidosqualene cyclase and squalene-hopene cyclase, carbocation cyclization is initiated by a protonated Asp residue. The terpenoid protonation step is assisted by hydrogen bonding stabilization of the conjugated base of the catalytic acid residue.
Dihydrofolate reductase (*80–89*, *106*) (NADPH)	Catalyzes the hydride transfer between NADPH and 7,8-dihydrofolate.	A sequence of concurrent hydrogen binding interactions is enhanced along the hydride-transfer reaction coordinate. The M20 loop motion is essential for substrate and cofactor binding, product release, and maintaining a key hydrogen bonding network.
Enolase (*49–51*) (Mg^{2+}, Mg^{2+})	Catalyzes the conversion of 2-phospho-D-glycerate to phosphoenolate pyruvate by proton transfer from carbon to a lysine.	The energy cost for the proton abstraction from a carbon acid by a weak base (Lys residue) is provided by the energy gained as a result of increased electrostatic stabilization of the dianion intermediate by two active-site Mg^{2+} ions.
Haloalkane dehalogenase (*32*, *67*, *68*, *130*)	Catalyzes the nucleophic substitution of haloalkanes to convert them to alcohols.	Desolvation effects contribute about 6 to 8 kcal/mol to the reduction of activation barrier. In addition, transition state is more stabilized by two tryptophan residues than is the reactant state in the enzyme due to the development of charges on the leaving group.
Liver alcohol dehydrogenase (*71*, *106*, *116*) (NAD^+)	Catalyzes the reversible transformation of an alcohol to an aldehyde.	A network of hydrogen bonding interactions facilitates the deprotonation of an alcohol substrate bounded to a Zn^{2+} ion. One of the α-hydride ions of the alcoholate anion is transferred to the cofactor NAD^+. Inclusion of tunneling contributions is essential to rationalize the observed kinetic isotope effects.
Methylamine dehydrogenase (*105*, *110*, *111*, *113*, *115*) (TTQ)	Catalyzes the oxidative conversion of primary amines to aldehyde and ammonia. The mechanism involves a proton transfer between aspartate and a methyliminoquinone intermediate.	The reaction involves a formal proton abstraction from a carbon acid by a weak base (Asp residue). The enzyme converts the alkyl amine into a protonated Schiff base through the TTQ cofactor (which is formed from two Trp residues). This substantially increases the acidity of the carbon acid, and the transition state is stabilized by the formation of an intramolecular zwitterion.
MutT pyrophospho-hydrolase (*36*) (Mn^{2+}, Mg^{2+})	Catalyzes the hydrolysis of nucleoside triphosphates.	The divalent Mn^{2+} ion, which is bound to the enzyme, activates a water molecule for nucleophilic attack, and electrostatic interactions with the second divalent ion provide stabilization of the pyrophosphate ion product. An active side residue (Asp^{53}) is the base that removes a proton from the nucleophilic water molecule.
Orotidine 5′-monophosphate decarboxylase (*27*, *73–76*)	Catalyzes the exchange of CO_2 for a proton at the C6 position of orotidine 5′-monophosphate.	Conformational change of the enzyme from a less stable conformation in the reactant state, induced by binding of the substrate, to a more stable form at the transition state is suggested as a main factor in reducing the barrier. The transition state is also stabilized by electrostatic interactions with a Lys residue, initially hydrogen bonded to the ribosyl 2′-hydroxyl group.

Table 1. Continued.

Enzyme*	Function	Mechanism
Protein tyrosine phosphatase (*52–56*)	Catalyzes the dephosphorylation of tyrosine phosphate via an S_N2 displacement of the phosphate thioester by cysteine.	Transition-state stabilization by enhanced hydrogen bonding interactions is achieved through geometrical changes in going from a tetrahedral structure to the trigonal bipyramidal configuration. The increase in the bond lengths of apical oxygen atoms of the phosphate ion leads to shortening of hydrogen bonding distances to the phosphate-binding loop.
Soybean lipoxygenase (*112*, *115*) (Fe^{3+})	Catalyzes the oxidation of unsaturated fatty acids. The mechanism involves a hydrogen transfer between the substrate and a hydroxide ion ligated to Fe^{3+}.	Tunneling contributes substantially to the rate constant calculated for this enzyme.
Triosephosphate isomerase (*31*, *44*, *45*, *47*, *102*, *108*, *117*)	Catalyzes the interconversion of dihydroxyacetone phosphate and (*R*)-glyceraldehyde 3-phosphate via proton-transfer reactions.	Electrostatic interactions with Lys^{12}, the neutral His^{95}, and other mainly charged residues reduce the transition-state barrier for the reaction in the enzyme by 11 to 13 kcal/mol.
Tyrosyl–tRNA synthetase (*20*, *34*)	Catalyzes the cleavage of the glycosylic bond between uracyl and DNA, which yields a sugar cation and uracilate anion.	Enzyme–transition state and enzyme-intermediate complementarity help to stabilize the transition state of tyrosine activation and to shift the chemical equilibrium by seven orders of magnitude in the direction of the intermediate. Loop motions induced by the chemical process are essential in creating these interactions and permitting access to the active site.
Xylose isomerase (*90–92*) (Mg^{2+}, Mg^{2+})	Catalyzes the interconversion between aldose and ketose sugars via an intramolecular hydride-transfer mechanism.	The transition state of the hydride-transfer reaction is stabilized by electrostatic interactions with two Mg^{2+} ions in the active site. Concerted motions of one of the metal ions accompanying the hydride-transfer reaction are critical for achieving a protein conformation that stabilizes the transition state.

*Cofactor, if any, is shown in parentheses.

rate due to the other major quantum effect, namely tunneling, is given by $\kappa(T)$ (*5–7*, *9*). The third contributing factor, $g(T)$, arises from deviations of the equilibrium distribution in phase space; $g(T)$ can be either less than or greater than 1; i.e., there can be either an enhancement or a decrease of the reaction rate relative to that which would exist when all degrees of freedom have their equilibrium (Boltzmann) distribution (*16–18*).

We note that the quantitative separation of the effects embodied in Eq. 1b is very difficult (if not impossible) by experiment, so that a clear understanding of the contributions to $\gamma(T)$ is best obtained from theory and simulations. Theoretical analyses lead to a deeper understanding of enzyme catalysis than can experiment, because the former provides access to details of the underlying mechanism that are not available from the latter. However, because of the approximations in the calculations (i.e., the nature of the potential energy function and the method used for calculating the reaction rates), it is important to test the results by comparisons with experiments, as far as they go (*12*).

Application to enzyme kinetics. In the application of Eq. 1 to the mechanisms of enzymatic rate acceleration, one is confronted with the fact that many enzyme reactions have multiple intermediates (*19*, *20*). Thus, it could be argued that it is necessary to treat the entire range of kinetic schemes that have been described (*21*). However, for our purpose, it is sufficient to consider the Michaelis-Menten formulation (*20*), which is widely used to provide a phenomenological description of enzyme mechanisms,

$$E + S \overset{K_S}{\leftrightarrows} ES \overset{k_{cat}}{\rightarrow} E + P \qquad (2)$$

In Eq. 2 the reaction is divided into two steps: The first is the formation of the enzyme substrate complex, ES, from the enzyme, E, and the substrate, S, with the equilibrium binding constant K_S, and the second is the chemical step corresponding to the formation of product P with a rate constant k_{cat}. Given Eq. 2, we have two limiting cases. If the substrate concentration is sufficiently high so that the enzyme is completely saturated (i.e., only the ES complex is present in solution), the rate of the enzyme-catalyzed reaction is given by

$$\text{Rate} \sim k_{cat}[E]_0 \qquad (3)$$

where $[E]_0$ is the total enzyme concentration,

$$[E]_0 = [E] + [ES] \sim [ES] \qquad (4)$$

If the substrate concentration is low ($[S] \ll K_S$), we have

$$\text{Rate} \sim (k_{cat}/K_S)[E]_0[S] \qquad (5)$$

For cases corresponding to Eq. 3, k_{cat} is of primary interest, the reaction is unimolecular, and the relevant activation free energy is the free energy difference between the enzyme-bound transition state and the ES complex; when Eq. 5 is applicable, the ratio k_{cat}/K_S is the essential quantity, the reaction is bimolecular, and the relevant activation free energy is the free energy difference between the enzyme-bound transition state and that of free E and S in solution. In writing Eq. 3, it is assumed that all binding and release steps are fast relative to k_{cat}. Even if they are not (for example, in many enzymatic reactions, product release or substrate binding is the rate-limiting step; this is often referred to as "kinetic complexity" in the enzyme literature), it is still of importance to study k_{cat}. Its analysis provides an understanding of the key chemical question, namely, how the rate of the chemical step has been accelerated to make it comparable to or faster than the other steps in the overall reaction, even when this step is so fast [a "perfect enzyme" in the colorful terminology of Knowles and Albery (*22*)] that it is no longer rate limiting. Thus, when more complex reaction schemes are required (*21*), they do not affect the significance of the present analysis.

Enzymatic reactions are often characterized in the literature by a phenomenological free energy of activation, with the rate constant written as

$$k(T) = (k_B T/h)(C^0)^{1-n} \exp[-\Delta G^0_{act}(T)/RT] \qquad (6)$$

where ΔG^0_{act} is by definition the phenomenological standard-state molar free energy of

activation obtained from a measurement of $k(T)$ at a single temperature (T). Given this convention, it is of interest to express the contributions to the transmission coefficient in energy units. Such a formulation is implicit in the free energy diagrams that are widely used to describe enzymatic reactions (*3*, *20*, *23*, *24*). We have

$$\Delta G_{\text{recross}} = -RT \ln \Gamma(T) \quad (7)$$

$$\Delta G_{\text{tun}} = -RT \ln \kappa(T) \quad (8)$$

$$\Delta G_{\text{noneq}} = -RT \ln g(T) \quad (9)$$

with the overall rate constant of the reaction given by

$$k(T) = (k_B T/h)(C^0)^{1-n} \exp\{[-\Delta G^{\text{TS},0}(T) - \Delta G_{\text{extra}}(T)]/RT\} \quad (10)$$

where the "extra-thermodynamic" term, ΔG_{extra}, is given by

$$\Delta G_{\text{extra}} = \Delta G_{\text{recross}} + \Delta G_{\text{tun}} + \Delta G_{\text{noneq}} \quad (11)$$

and

$$\Delta G^0_{\text{act}} = \Delta G^{\text{TS},0} + \Delta G_{\text{extra}} \quad (12)$$

Applying Eq. 6 to the limiting cases for enzymatic reactions given in Eqs. 3 and 5, we see that Eq. 3 corresponds to Eq. 6 with $n = 1$ (unimolecular) and Eq. 5 to Eq. 6 with $n = 2$ (bimolecular); we note that $\Delta G^0_{\text{act}} \neq RT$ has a different meaning in the two cases.

Lowering the Quasithermodynamic Free Energy of Activation ($\Delta G^{\text{TS},0}$ in Eq. 1a)

Studies of enzymes show that natural selection has developed many ways for lowering the quasithermodynamic activation free energy. In what follows, we do not aim to make an exhaustive survey, but rather to describe selected examples that are well understood through computational modeling and experiment and that illustrate essential aspects of enzyme catalysis.

The catalytic effect of an enzyme has been defined as "the ratio between the reaction rate in the presence of enzyme and the rate of a reference reaction" [(*25*), p. 12]. Often one takes the reference reaction as that in aqueous solution (*26*–*29*). It should be noted, however, that an enzyme can make a reaction proceed by a different mechanism than the one operating in solution (*30*). In many cases the mechanism is unchanged, and computational studies can provide quantitative comparisons of the rates for the same reaction in aqueous solution and in the enzyme. Additional insights have been obtained from calculations that compare the results for the enzyme with those in the gas phase, as well as in solution (*31*–*33*).

The most widely used experimental approach for determining how the activation free energy is lowered is protein engineering; i.e., comparison of the rate in a mutant to that in the wild type. There are many examples of this type of approach, which was initiated by Winter and Fersht in their pioneering analysis of tyrosyl–tRNA synthetase (*20*, *34*). Recent successful examples of protein engineering include the study of the role of steric bulk of one amino acid in controlling the reaction catalyzed by cycloartenol synthase (*35*), the study of the effect of charged residues on bimetallic catalysis in MutT pyrophosphohydrolase (*36*), and the differential stabilization of the transition state with respect to the reactant state in the chorismate mutase reaction due to a charged arginine residue (*37*). In the third system, the authors made an isosteric substitution to try to separate structural from electrostatic features and reactant from transition state features. This led to an estimate of 6.5 kcal/mol for the electrostatic contribution to lowering the transition-state free energy. Even in such careful experimental work, it is hard to prove that the separation was actually achieved because the measured rates and equilibrium constants reflect all effects on both species, whereas in computer simulations, one can verify such assumptions, as we show below. Other problems that can arise in the interpretation of experimental mutant studies have been described (*38*–*40*).

Analyses of enzyme catalysis by computer simulations are providing a detailed understanding of how the activation barrier is lowered, including a delineation of the contributions made by the structure of the enzyme and by its flexibility. The former provides a "pre-organized environment" (*41*) that enhances catalysis (either statically or by means of the changes that occur along the reaction pathway from reactants to the transition state, or both) by providing a stronger stabilization of the transition state than of the reactant state (which can be the bound enzyme-substrate complex, as in Eq. 3, or the free enzyme and substrate, as in Eq. 5). Such a preorganized active site can lead to contributions to catalysis from interactions with the bound substrate (*42*) or with the bound product of one step of a reaction that serves as the reactant in the next step (*43*), as well as from the enzyme itself. If the difference between the reactant state and transition state involves substantial charge transfer, as it does in many enzymatic reactions, the positions of the polar and charged groups in the enzyme (including metal ions and cofactors, when present) play the essential role. Hydrogen bonding, which is typically dominated by electrostatics, is often used in combination with other electrostatic effects to stabilize the transition state. However, electrostatic effects are not always dominant; see, for example, the discussion of the Co corrinoid mutases given below. A certain degree of enzyme flexibility is essential for catalysis; i.e., some atomic motions in the enzyme are involved in most reactions (*12*). Moreover, larger scale motions also can be involved in catalysis, as well as in providing a protected catalytic site while permitting the substrate to enter and the product to escape. It is important to note that changes in enzyme structure and vibrational modes associated with the progress of the reaction often promote catalysis most efficiently by lowering the quasithermodynamic free energy barrier. This effect is distinct from the role of such motions in the generalized transmission coefficient, which is discussed in the next section.

One of the enzymes in which electrostatic effects are dominant is triosephosphate isomerase (TIM), a dimer that catalyzes the conversion of dihydroxyacetone phosphate (DHAP) to (*R*)-glyceraldehyde 3-phosphate (GAP). The apparent barrier for the reaction in the enzyme has been calculated to be 11 to 13 kcal/mol lower than that for the reaction in aqueous solution (*31*, *44*). A detailed computational analysis of the contributions of individual residues to the various steps in the reaction catalyzed by the enzyme has been made, and their role in alternative reaction mechanisms has been elucidated (*45*). The rate-determining step is the transfer of a proton from DHAP to Glu^{165}, and the residue contributions to lowering the activation energy of this step are shown in Fig. 1A; the calculated positions of important residues in the active site are shown in Fig. 1B. The charged residue Lys^{12} makes the most important contribution, but the neutral His^{95} side chain as well as certain main-chain NHs also contribute (*46*). A "lid" motion has been demonstrated to be involved in making the active site of TIM accessible and closing it off for catalysis (*47*). A smaller lid motion occurs in aminotransferases, where the free energy difference between the open and closed form has been estimated to be 2 kcal/mol (*48*).

Another enzyme for which the importance of electrostatic effects has been demonstrated by calculations is enolase (*49*–*51*). Enolase abstracts a proton from a carbon acid by use of a weak base (Lys) to produce a $RCH{=}CO_2^{2-}$ species. Lowering the activation barrier for the abstraction reaction corresponds to equalizing the large pK_a difference between the carbon acid and Lys. Model calculations have estimated that the energy to achieve a nearly thermoneutral reaction in the enzyme is about 290 kcal/mol, relative to the gas-phase bimolecular reaction (*50*). The predominant contribution to lowering the barrier for the proton-abstraction reaction (estimated roughly as 56 kcal/mol) arises from electrostatic interactions of the doubly

anionic enolate with two Mg^{2+} ions, relative to the interactions of the singly anionic carboxylate reactant.

An example involving hydrogen bonding is provided by the protein tyrosine phosphatase (*52*, *53*), which catalyzes the hydrolysis of proteins phosphorylated at tyrosine residues; an experimental analysis of the mechanism of this enzyme (*54*) is consistent with the role of hydrogen bonding in transition-state stabilization. The process begins with a nucleophilic attack by a cysteine thiolate anion at phosphorus to yield a covalent phosphothiolester intermediate, followed by nucleophilic substitution by a water molecule. Both steps involve Walden inversion of configuration at phosphorus. There is no metal ion present in the active site, and the stabilization of the transition state by nucleophilic substitution is provided, in part, by hydrogen bonding interactions with the anion-binding loop. The change of the phosphorus center from a tetrahedral structure at the reactant state to a trigonal bipyramidal geometry at the transition state extends the three oxygen atoms of the phosphate toward the anion-binding loop, which is relatively rigid, resulting in shorter hydrogen bond distances and stronger interaction energies at the transition state relative to that in the Michaelis complex by 5 to 6 kcal/mol (*53*). Free energy simulations reveal that hydrogen bond distances between the oxygen atoms of the phosphate and the anion-binding loop are shortened by 0.05 to 0.10 Å on average in going from the reactant to the transition state. The computational results are mirrored by the observation that average reductions of 0.12 to 0.18 Å in hydrogen bond distance were found in the equatorial oxygens of the vanadate transition-state analog compared to phosphate and sulfate ions in x-ray structures of the complexes (*55*, *56*).

Additional examples showing the central importance of the lowering of the free energy barrier by enzymes include the studies of the flavoprotein monooxygenases, phenol hydroxylase, and parahydroxybenzoate hydroxylase, in which a specific transition-state stabilization interaction was identified by modeling and subsequently confirmed by experiment (*57*, *58*). Another example is provided by glutathione transferase, in which analysis of the effects of mutations indicated a specific residue affecting the barrier as a key determinant of stereospecificity in the enzyme-catalyzed epoxide ring opening (*59*).

Chorismate mutase, which catalyzes an essential step in the synthesis of the aromatic amino acids Trp, Tyr, and Phe, has become very popular for theoretical studies of enzyme catalysis, as judged by many recent publications (*60*). The enzyme is of particular interest because there are two primary contributions to the lowering of the activation free energy. The first, similar in character to that in TIM, involves electrostatic stabilization of the transition state, which lowers the free energy of activation by several kcal, as already mentioned (*37*, *61*, *62*). More unusual is the additional contribution that arises owing to the stability of an inactive conformation in solution (Fig. 2A); the enzyme binds this conformation and transforms it to the active conformation (Fig. 2B) (*63*, *64*). The conformational stabilization of the latter has been estimated by free energy simulations to contribute about 5 kcal/mol, in agreement with the analysis of mutation results (*64*). "Reactant destabilization" and "near-attack conformers" (NACs) (*65*) have been invoked for this case, but the essential effect is that the activation free energy barrier is reduced by the substrate conformational change induced by the enzyme [see also (*97*)].

Chemical reactions can be strongly influenced by the media in which they take place, and desolvation has been used to explain experimental results on S_N2 reactions (*23*); e.g., the fact that the reactant is better solvated than the transition state increases the activation energy in solution relative to that in the gas phase (*66*). In the haloalkane dehalogenase reaction (*32*, *67*, *68*) (one step of which is an S_N2 displacement of a chloride ion by a carboxylate of an Asp residue), the Asp carboxylate and the substrate in the active site are well positioned for reaction. In aqueous solution, there is an appreciable penalty for removing water molecules that are solvating the carboxylate group, whereas in the enzyme, the environment is such that the

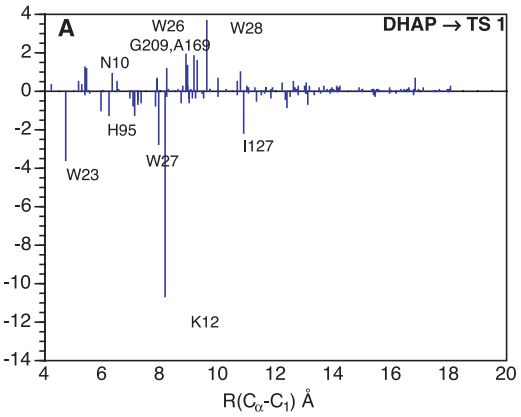

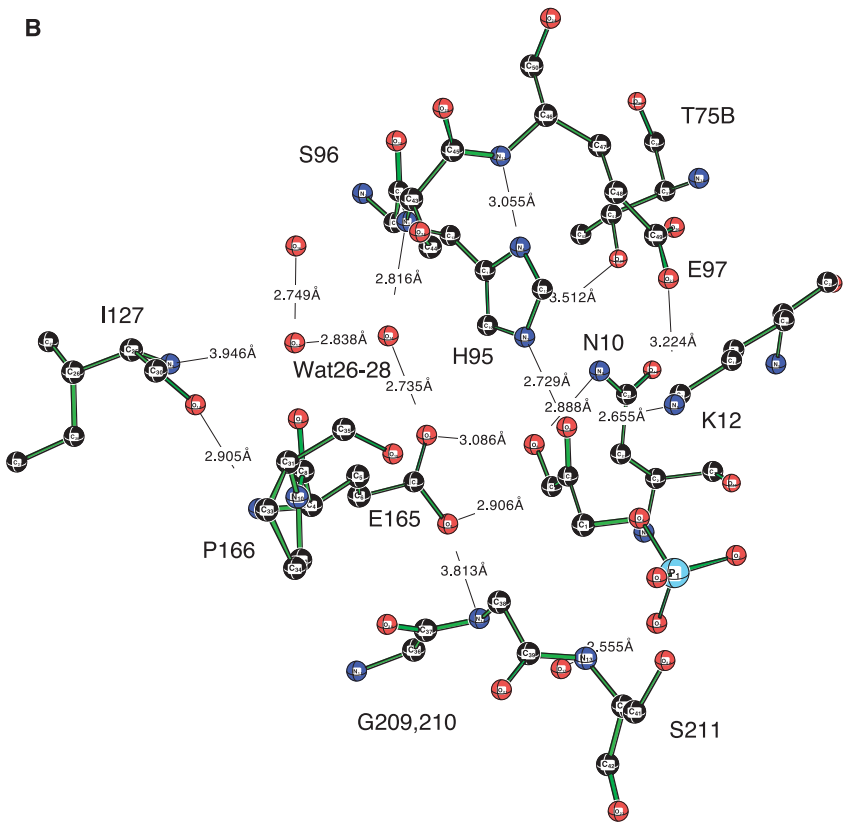

Fig. 1. Triosephosphate isomerase. (**A**) Electrostatic contribution of individual residues (in kcal/mol on the ordinate) to the lowering of the activation energy barrier (TS1) of the reaction of the DHAP substrate to form the enolate intermediate. This is the rate-determining step of the overall chemical reaction. The residues are plotted on the abscissa as a function of the distance from the Cα carbon of the residue (or the oxygen of a water molecule, W) to C_1 of the substrate. Negative values correspond to lowering of the barrier. (**B**) Active-site structure at transition state showing important residues and water molecules.

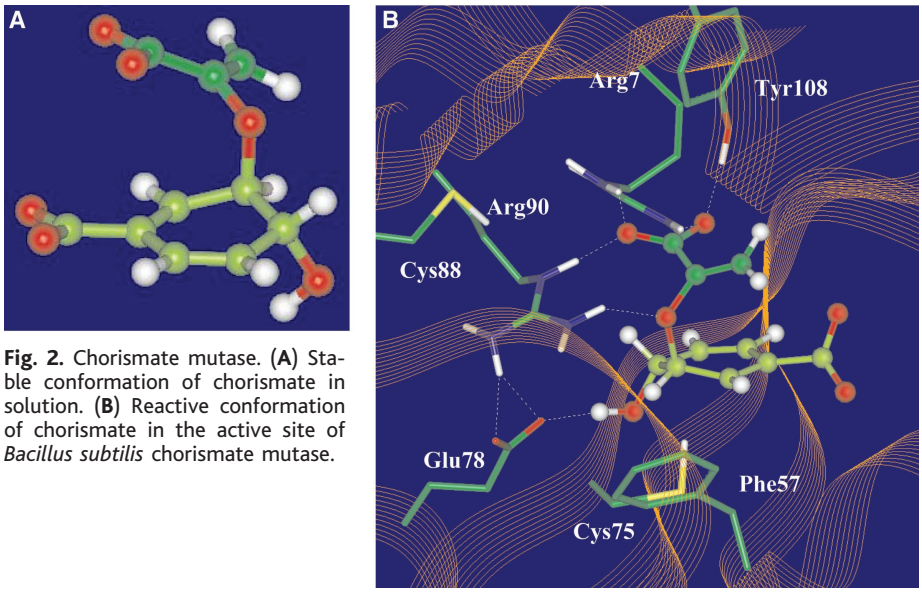

Fig. 2. Chorismate mutase. (**A**) Stable conformation of chorismate in solution. (**B**) Reactive conformation of chorismate in the active site of *Bacillus subtilis* chorismate mutase.

solvation penalty is considerably smaller. Two computational estimates of the difference in solvation free energy between aqueous solution and the enzyme are 6 kcal/mol (*67*) and 8 kcal/mol (*32*). In addition, hydrogen bonding interactions between two tryptophan residues and the chloride ion leaving group stabilize the transition state by about 8 kcal/mol (*32*).

Enzyme relaxation and conformational change. It is important to remember that $\Delta G^{TS,0}$ includes the conformational free energy of the enzyme, as well as that of the substrate (*3*). (For the latter, estimates between 1.3 and 3.2 kcal/mol as the contribution from substrate vibrations to the lowering of the activation free energy have been made (*69*–*71*). The enzyme free energy at the transition state can be different from that in the reactant state, so that conformational changes can contribute to lowering or increasing the activation barrier. In the calculations we have described so far, such effects are included, but they have not been separated from the other contributions. The effect of the relaxation of the protein along the reaction path (between reactant and transition state) has been estimated for liver alcohol dehydrogenase (LADH) (*72*) and short-chain acyl–coenzyme A (CoA) dehydrogenase (*73*). In both systems, the effective potential along the substrate reaction coordinate with the enzyme frozen was calculated. Then, the enzyme was allowed to move, and a free energy perturbation method was used to obtain the sum of the change in the internal free energy of the protein and its interaction free energy with the substrate along the reaction path. In the first case, it was estimated that the relaxation of the enzyme stabilizes the system by less than 2 kcal/mol, whereas in the second case, a stabilization of 18 kcal/mol was estimated.

The enormous catalytic efficiency of orotidine monophosphate (OMP) decarboxylase (ODCase) has attracted numerous experimental and computational investigations (*27*, *74*–*76*). The ODCase reaction appears to be another case in which the enzyme itself is more stable in the transition state than in the reactant state, thereby contributing to the lowering of the activation free energy. To demonstrate this lowering, the difference in the free energy barrier between the catalyzed and aqueous (uncatalyzed) reaction has been decomposed into the change, ΔG_1, in interaction energy between the substrate OMP and its environment and the change, ΔG_2, in the environmental free energy accompanying the chemical transformation. By umbrella sampling (*77*), it was estimated that $\Delta G_1 + \Delta G_2 = -22$ kcal/mol, whereas perturbation techniques yielded a value for ΔG_1 equal to -2 kcal/mol. Consequently, the change in the internal free energy of the enzyme is about -20 kcal/mol in going from the reactant structure to the transition state, resulting in an overall transition state barrier of 15 kcal/mol. Apparently, a strain induced in the enzyme by substrate binding is relieved only at the transition state (fig. S1).

The Co corrinoid mutases (*78*, *79*) are enzymes in which x-ray structural data indicate that conformational change and steric effects are important in lowering the activation free energy. They are TIM barrel proteins in which binding of the substrate induces a major conformation change in the barrel, which is hinged in this case. In addition to being involved in substrate binding and product release, the conformational change induces a movement of a tyrosine residue (Tyr^{A89}) across the Co-C bond, sterically pushing the carbon center (which is the 5′ carbon of 5′-deoxyadenosylcobalamin) off the Co. The carbon radical so produced abstracts a hydrogen atom from the methyl group of the substrate to initiate a free radical mechanism for a carbon skeletal isomerization with a much lower $\Delta G^{TS,0}$ than if it were still bonded to Co in the reactant of the rate-determining step. Also, a large number (30 or so) of waters are released, which is expected to provide an entropic contribution to catalysis. Calculations (*80*) support the interpretation from the x-ray data and provide additional insights; in particular, they have shown that Arg^{207} promotes the first step by hydrogen bonding to the substrate carbonyl group, and that the second step is dominated by tunneling.

Dihydrofolate reductase (DHFR) catalyzes the hydride transfer between nicotinamide adenine dinucleotide phosphate (NADPH) and 7,8-dihydrofolate (DHF). Structural (*81*) studies showed that the M20

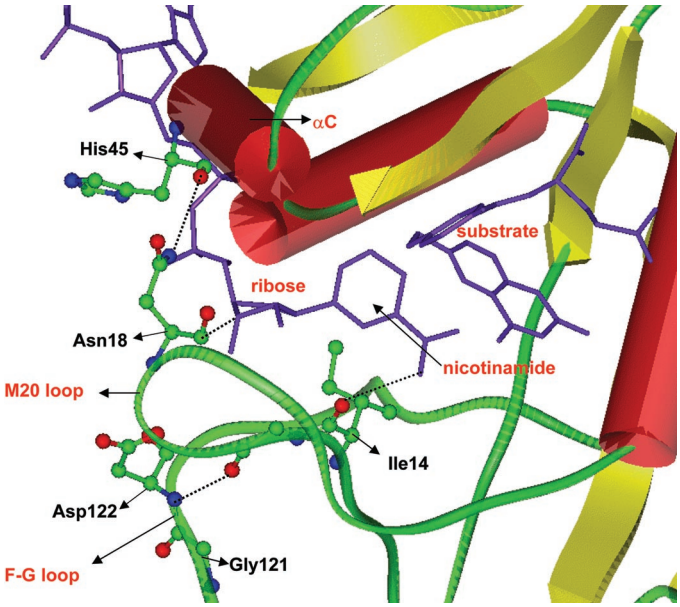

Fig. 3. Dihydrofolate reductase (DHFR). Partial view of the DHF-NADPH-DHFR complex. The residues that are cited in the text because they interact with the cofactor (NADPH in violet) are shown in ball-and-stick representation (in green for C, blue for N, and red for O). The analysis of average hydrogen bond distances along the hydride-transfer reaction for structures generated by molecular dynamics simulation suggests that, in going from the reactant to the transition and product states, the M20 loop residues (10 to 24) approach to the cofactor, whereas the interaction between them and the F-G loop (residues 116 to 125) decreases.

loop (residues 10 to 24, Fig. 3) of *Escherichia coli* DHFR can adopt several conformations, and nuclear magnetic resonance (*82*) experiments revealed that it oscillates at a frequency similar to k_{cat}. It has been proposed that an "open" M20 loop conformation is essential for substrate and coenzyme binding and for products release, which is the rate-limiting step (*83*), whereas the closed M20 conformer is required for the chemical step. In this conformation, the M20 loop has specific interactions with the nicotinamide and ribose groups of the cofactor, with the F-G loop (residues 116 to 125, Fig. 3), and with helix C (residues 44 to 55, Fig. 3) that stabilize the cofactor in a proper conformation for reacting with the substrate. A recent computational study (*84*) demonstrates that the barrier height for the hydride transfer is increased by the mutation of a residue in the F-G loop (19 Å from the reaction center), in agreement with experimental results (*85*). Agarwal *et al.* (*86*, *87*) have described the change of hydrogen bonding distances along the hydride-transfer reaction path in DHFR as coupled "promoting" motions that provide stabilization of the transition state. These coupled motions reflect the structural response by the enzyme to the changes of the substrate in geometry and electronic structure, or vice versa. We note that such motions are included in the quasithermodynamic free energy of activation (Eq. 1a) and are an intrinsic part of the protein dynamic fluctuations during the chemical process. The computational studies indicate, either indirectly through analysis of geometrical changes along the reaction path (*86*–*89*) or directly by electrostatic analysis (*88*), that the transition state is stabilized by residues in the M20 loop and other loops that are not hydrogen bonded to the substrate or coenzyme (i.e., "distant" residues), as well as by residues at the active site. This is consistent with site-directed mutagenesis experiments (*90*); however, the simulations provide many details that are inaccessible to experiment. For example, a distant residue in the F-G loop (Asp^{122}, Fig. 3) helps stabilize the transition state through a 3.5-kcal/mol long-range electrostatic interaction (*88*).

In xylose isomerase, the enzyme adopts different conformations in the reactant state and in the transition state, and the change in conformation makes an important contribution to $\Delta G^{TS,0}$. The hydrogen-transfer reaction coordinate is coupled to a coordinate involving the motion of Mg^{2+} ions in the active site. The motion of Mg2 (Fig. 4), in particular, promotes a charge-transfer step through first ligand shell coordination. A simulation study (*91*, *92*) of xylose isomerase shows that the metal motion is correlated with the hydride-transfer reaction coordinate, as well as with a change in the length of a key hydrogen bond (O1-Lys^{182} in Fig. 4). Figure 4 illustrates the correlation between changes in geometry and atomic partial charges. Computer simulations (*93*) starting from two different x-ray structures of the enzyme indicate that the movement of the metallic cofactor is very sensitive to subtle differences in its coordination sphere; i.e., the movement, which has been inferred from x-ray data, is reproduced in only one of the simulations. The transition-state configurations in the latter have a shorter oxygen-lysine distance (O1-Lys^{182}), and it gives a value of $\Delta G^{TS,0}$ that is 5 kcal/mol lower than that of the other simulation, providing a quantitative estimate of the effect of the structural change in catalysis.

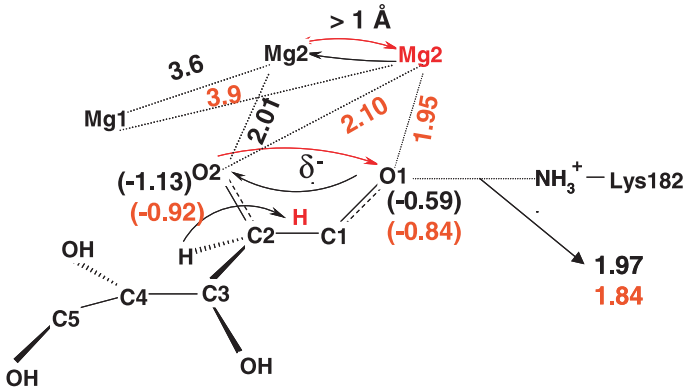

Fig. 4. Xylose isomerase. Schematic representation of the main changes that accompany the hydride-transfer reaction in the active site. Dynamical fluctuations of the Mg2 ion between two different positions in the active site modulate the charge migration from O2 to O1 atoms of xylose. The red arrows indicate the direction of the charge migration that favors the hydride shift from C2 to C1. Averaged distances (in A) for important interactions and the charges on the oxygens (in parentheses) at the reactant (black) and at the transition state (red) are indicated. The development of negative charge on O1 enhances the strength of the hydrogen bond between the substrate and Lys^{182}, which also contributes to the transition-state stabilization.

Analyses of enzyme catalysis not involving the transition state. Some workers have focused on the bound reactant (reactant destabilization) or on configurations along the reaction path before the transition state is reached. For example, Bruice and co-workers (*71*, *94*, *95*) have emphasized the stabilization (relative to the reactant geometry free in solution) of what they call near-attack conformers (NACs). Similarly, Young and Post (*96*) have pointed to the putative restriction of the substrate conformations to structures similar to the transition state and the resulting increase in the free energy of reactant, which results in lowering of the entropic contribution to the free energy of reaction, an effect that they refer to as "entropic guidance." Such studies focus on configurations in the "foothills" rather than at the top of the barrier. Although information about the stabilization of the NACs, for example, can be a useful indication of how the transition state is stabilized, it does not provide a way of determining $\Delta G^{TS,0}$, the essential quantity (*97*). A related approach is to compare the free energy gain in forming the Michaelis complex to the free energy cost [sometimes called the cratic free energy (*98*, *99*)] for preorganizing the substrate in solution. This component of catalysis needs to be recognized as only one part of the free energy difference between the reactants and the transition state.

Role of Transmission Coefficient [$\gamma(T)$ in Eq. 1b]

The generalized transmission coefficient can be written as a product of three contributions, as shown in Eq. 1b. We discuss each of these in turn and evaluate their roles in enzyme catalysis.

Recrossing factor, $\Gamma(T)$. The first factor in Eq. 1b, $\Gamma(T)$, arises from dynamical recrossing; i.e., not all trajectories that cross the transition state in the direction of products contribute to the reaction rate, so that $\Gamma \leq 1$, where the value of unity corresponds to the transition-state theory limit. Such recrossing occurs, for example, because a trajectory starting in the reactant well is reflected on the product side of the transition state by forces due to the enzyme or solvent or by internal forces arising from the substrate itself. The essence of finding a good reaction coordinate and a good location for the transition state along that coordinate is to minimize the likelihood that such recrossing will occur; i.e., the transition state should be the "bottleneck." There has been concern about $\Gamma(T)$ in enzyme for a long time (*100*, *101*), but it is only recently that simulations have been able to estimate its magnitude (*70*, *102*). It is possible that $\Gamma(T)$ is larger or smaller for the enzymatic reaction than for the corresponding reaction in solution. One reason for it to be smaller is that the nature of the enzyme environment and the importance of interactions with specific residues might cause the true dynamical bottleneck to be a complicated function of the system coordinates; as a result, a simple reaction coordinate, such as that used in (*102*), would lead to a dividing surface with substantial recrossing.

$\Gamma(T)$ has been calculated for reactions in the gas phase, in solution, and recently in certain enzymes. One method (*8*) used for

enzymes (*102*) is based on classical dynamics, in which a large number of trajectories are started in the transition-state region, all initially going from reactant to product. These trajectories are followed both forward and backward in time until the system is trapped in either the product or reactant state. $\Gamma(T)$ has been estimated (*102*) as 0.4 for the initial proton-transfer step from the DHAP substrate to Glu^{165} for the enzyme triosephosphate isomerase by treating the dynamics as purely classical. Using the same computational approach, $\Gamma(T)$ values of 0.53 and 0.26 have been obtained, respectively, for the enzymatic nucleophilic substitution reaction of dichloroethane and Asp^{124} in haloalkane dehalogenase and for the corresponding uncatalyzed process in water (*103*). For most uncatalyzed reactions in liquid solution, $\Gamma(T)$ is between 0.5 and 1 (*9*), only slightly smaller than that calculated for many gas-phase reactions at room temperature (*104*). With quantum mechanical approaches, values of $\Gamma(T)$ in the range 0.75 to 0.95 have been obtained for other enzyme-catalyzed reactions (*72*, *86*, *88*, *92*, *105*, *106*); that $\Gamma(T)$ is closer to unity when quantization is included is in accord with results for simple reactions (*107*). We note that for LADH (*72*, *106*) and DHFR (*86*, *88*), two different approximate quantum mechanical approaches with different definitions of the reaction coordinate gave very similar values (near unity) for $\Gamma(T)$. The good agreement for these two cases, especially DHFR for which changes in average protein conformations from the Michaelis complex to the transition state have been observed experimentally and computationally, provides evidence that fluctuations of complex enzyme systems do not automatically invalidate the use of simple reaction coordinates either for framing discussions or for quantitative calculations; i.e., the effect of protein conformational changes is included in $\Delta G^{TS,0}$. Overall, we have learned from the recent simulations that, although the recrossing factor is quantitatively interesting in terms of a full understanding of the reaction, the magnitude of its effect is often small as compared with other contributions.

Tunneling factor, $\kappa(T)$. Considerable attention has focused recently on the contribution of tunneling in enzymatic reactions, particularly those involving hydrogen (hydrogen atom, proton, hydride ion) transfer (*69*, *108*–*111*). The pre-exponential factor $\kappa(T)$ is the factor that determines the tunneling contribution to the reaction. Because inferences about the magnitude of $\kappa(T)$ from experiment are indirect (*112*–*114*), simulations including quantum effects are essential for a direct determination of this quantity. Calculations (at room temperature) yield rate enhancements due to tunneling of 1.5 for the intermolecular transfer in TIM (*108*) to 23 to 114 for methylamine dehydrogenase (*105*, *110*, *111*, *115*), and 780 for soybean lipoxygenase (*115*), for example. These accelerations are equivalent to free energy effects (by Eq. 8) of 0.2 to 3.9 kcal/mol. Tresadorn *et al.* (*115*) explained the large differences among three enzymes by a detailed comparison of the shapes of their effective barriers, the curvatures of their reaction paths, and the relative displacement of barrier features and curvature features with respect to each other. Similar analyses for TIM and LADH were used to explain the kinetic isotope effects and Swain-Schaad exponents (*72*, *108*, *116*, *117*).

Zero-point contributions (included in the quasithermodynamic activation free energy) and tunneling are both quantum effects that are important in calculating the rate of a reaction. The former are likely to be similar in enzymes and solution and, therefore, make a relatively small contribution to catalysis, as pointed out in the previous section. However, tunneling can be more important than zero point effects for catalysis because the slow step in uncatalyzed reaction in aqueous solution is often very endothermic. Highly unsymmetric reactions tend to have small intrinsic barriers (the intrinsic barrier is the barrier in the downhill direction) and thus have little tunneling. For example, the formal reaction (hydride transfer from an alcoholate anion to NAD^+) catalyzed by LADH is highly exothermic in the gas phase and in water; the enzyme actually raises the barrier of the hydride-transfer step to make it closer to thermoneutral. In cases where the reaction is more thermoneutral in the enzyme than in aqueous solution, it is likely to have a more symmetric and thinner barrier, so that tunneling could make a small, but nonnegligible, contribution to catalysis. An alternative scenario is that the reaction energy does not change but that the barrier is lower; in such cases, the barrier will tend to be broader and tunneling will compete less well with overbarrier processes in the enzyme than in aqueous media, making a negative contribution to catalysis.

Nonequilibrium factor, $g(T)$. One classification of the deviations from transition state theory in condensed media (*7*) separates effects associated with the conversion of transition states into products and effects associated with the rate of creation of transition states. The former are included in $\Gamma(T)$, already discussed, whereas the latter are encompassed in $g(T)$. The idea that enzymes have certain vibrational degrees of freedom that are able to "store up" energy and then "channel" it into the reaction coordinate is very appealing and has often been discussed (*100*, *101*, *118*). For example, deviations from an equilibrium distribution of reactant states could, in principle, occur because substrate binding might convert large amounts of potential energy into kinetic energy, but we expect, in general, that energy relaxation is so fast that any excess kinetic energy would be dissipated too rapidly to contribute to the chemical step. If the reactant-state degrees of freedom are at equilibrium, even though the reactant concentration is far from equilibrium, transition state theory may be applied. That some modes can be more effective at causing reaction than other modes is included in transition state theory. Correspondingly, alteration of the fluctuations of the enzyme by substrate binding so as to lower the barrier for reaction would be an equilibrium effect (*118*, *119*). Also, the suggestion that tunneling or classical barrier recrossing is promoted by a particular vibration of the reactants does not necessarily involve deviations from equilibrium.

To assess the likelihood that nonequilibrium effects play a role in enzyme catalysis, we briefly review what is known from studies of simpler gas-phase and liquid-phase reactions. For unimolecular reactions in the gas phase, a case that provides an analog of k_{cat} for enzymes, nonequilibrium effects are well known, and they make the reaction slower than it would be if the system degrees of freedom were at equilibrium (*120*). The most carefully studied cases arise from a fall-off from the high-pressure limit in the rate of the unimolecular reaction, when the collisions with the environment are not sufficient to keep the internal energy in the solute degrees of freedom at equilibrium (*121*). Considerable effort has been expended in trying to observe this regime in liquids, but there is only one reaction for which a detailed analysis gives evidence for a nonequilibrium effect, namely, the isomerization of cyclohexane in CS_2. The pressure dependence of the rate was measured, and it was found that the rate increases with increasing pressure (*122*); the most complete simulations for the reaction yield values of $g(T)$ in the range 0.34 to 0.47 (*123*). To be effective in catalysis, $g(T)$ would have to be nearer unity in the enzyme than in solution, so the actual effect is expected to be quite small.

Concluding Remarks

Evolutionary selection makes possible the development of enzymes that use a wide range of molecular mechanisms to facilitate reactions. Although, in principle, such rate enhancements could arise from lowering the quasithermodynamic free energy of activation or increasing the generalized transmission coefficient, the present analysis shows that the former plays the dominant role. In the transmission coefficient, recrossing events and nonequilibrium excitations appear to be unimportant, but tunneling can lead to a sizable contribution to rate enhancements. Overall, the lowering of the activation free energy

has been found to accelerate the reaction rate by more than a factor of 10^{11}, whereas the transmission coefficient contributes no more than a factor of 10^3 to the rate.

The developments of modern transition state theory and its application to enzymes by computer simulations described in this review make clear that the quasithermodynamic free energy of activation is the most important factor in enzyme catalysis. Moreover, alternative descriptions proposed as the source of enzyme catalysis are encompassed in modern transition state theory and do not require the introduction of new concepts.

References and Notes

1. R. Wolfenden, M. J. Snyder, *Acc. Chem. Res.* **34**, 938 (2001).
2. L. Pauling, *Chem. Eng. News* **24**, 1375 (1946).
3. R. L. Schowen, in *Transition States of Biochemical Processes*, R. D. Gandour, R. L. Schowen, Eds. (Plenum, New York, 1978), p. 77.
4. A historical overview of mechanistic enzymology, which serves as an excellent complement to the present analysis, was published recently by Bugg (*124*). He points out that many enzymologists continue to search for the "elusive additional mechanisms by which enzymes may achieve high rates of catalysis" (p. 488). The thesis of the present article is that modern simulations of transition states are a powerful tool for discovering these mechanisms and that all such mechanisms can be understood in terms of various contributions to Eq. 1a. In another complementary article published after the present review was submitted, Benkovic and Hammes-Schiffer (*125*) provide a perspective on the contributions to catalysis by focusing on the properties of DHFR.
5. H. Eyring, A. E. Stern, *Chem. Rev.* **24**, 2 (1939).
6. D. G. Truhlar, W. L. Hase, J. T. Hynes, *J. Phys. Chem.* **87**, 2884 (1983).
7. M. M. Kreevoy, D. G. Truhlar, in *Investigation of Rates and Mechanisms of Reaction*, C. F. Bernasconi, Ed., vol. 6 of *Techniques of Chemistry*, A. Weissberger, Ed. (Wiley, New York, 1986), part 1, pp. 13–95.
8. J. B. Anderson, *Adv. Chem. Phys.* **91**, 381 (1995).
9. D. G. Truhlar, B. C. Garrett, S. J. Klippenstein, *J. Phys. Chem.* **100**, 12771 (1996).
10. The term "quasithermodynamic," rather than simply "thermodynamic," is appropriate because the activated complex is a mathematical construct rather than a stable or metastable entity. The transition "state" corresponds to an ensemble of systems that has all degrees of freedom of the entire system except one, the reaction coordinate, which is fixed. Protein motions and dynamic effects are included in Eq. 1a, even though the language is quasithermodynamic. Readers should not be confused by the fact that some workers [e.g., (*106*)] use the word "dynamics" to refer to deviations of the transmission coefficient from unity; in this article, dynamics is used in the more general sense of atomic and molecular motions.
11. For solution reactions, the Kramers formulation of transition state theory (*126*) is widely used. The factor k_BT/h does not appear explicitly in the usual Kramers theory rate expression because it cancels part of the reactant partition function in the one-dimensional analysis (*127*) that is commonly used.
12. C. L. Brooks III, M. Karplus, B. M. Pettitt, *Adv. Chem. Phys.* **71**, 1 (1988).
13. C.-J. Tsai, K. Jordan, *J. Phys. Chem.* **97**, 11227 (1993).
14. B. Ma, S. Kumar, C.-J. Tsai, Z. Hu, R. Nussinov, *J. Theor. Biol.* **203**, 383 (2000).
15. B. C. Garrett, D. G. Truhlar, *J. Phys. Chem.* **83**, 1052 (1979).
16. B. Shizgal, M. Karplus, *J. Chem. Phys.* **52**, 4262 (1970).
17. R. K. Boyd, *Chem. Rev.* **77**, 93 (1977).
18. C. Lim, D. G. Truhlar, *J. Phys. Chem.* **89**, 5 (1985).
19. G. G. Hammes, *Biochemistry* **41**, 8221 (2002).
20. A. Fersht, *Structure and Mechanism in Protein Science: A Guide to Enzyme Catalysis and Protein Folding* (Freeman, New York, 1999).
21. D. B. Northrop, in *Mechanism of Enzyme Action*, *Part A*, D. L. Purich, Ed. (Wiley, New York, 1999), pp. 25–55.
22. J. R. Knowles, W. J. Albery, *Acc. Chem. Res.* **10**, 105 (1977).
23. F. Takusagawa, M. Fujioka, A. Spies, R. L. Schowen, in *Comprehensive Biological Catalysis*, M. Sinnott, Ed. (Academic, San Diego, CA, 1998), vol. 1, pp. 1–30.
24. P. A. Kollman *et al.*, *Acc. Chem. Res.* **34**, 72 (2001).
25. M. B. Hall *et al.*, *ACS Symp. Ser.* **721**, 2 (1999).
26. A. Warshel, *Computer Modeling of Chemical Reactions in Enzymes and Solutions* (Wiley, New York, 1991).
27. R. Wolfenden, *Science* **267**, 90 (1995).
28. S. J. Benkovic, *J. Biol. Chem.* **273**, 26257 (1998).
29. A. Warshel, J. Bentzien, *ACS Symp. Ser.* **721**, 489 (1999).
30. J. P. Richard, *J. Am. Chem. Soc.* **106**, 4926 (1984).
31. Q. Cui, M. Karplus, *J. Phys. Chem. B* **106**, 1768 (2002).
32. L. S. Devi-Kesavan, J. Gao, *J. Am. Chem. Soc.* **125**, 1532 (2003).
33. S. Marti, J. Andres, V. Moliner, E. Silla, I. Tunon, J. Bertran, *Theor. Chem. Acc.* **105**, 207 (2001).
34. G. Winter, A. Fersht, *Nature* **299**, 756 (1982).
35. S. P. T. Matsude *et al.*, *Org. Lett.* **2**, 2261 (2000).
36. T. K. Harris, G. Wu, M. A. Massiah, A. S. Mildvan, *Biochemistry* **39**, 1655 (2000).
37. A. Kienhofer, P. Kast, D. Hilvert, *J. Am. Chem. Soc.* **125**, 3206 (2003).
38. G. E. Narlikar, D. Herschlag, *Biochemistry* **37**, 9902 (1998).
39. S. J. Admiraal *et al.*, *Biochemistry* **40**, 403 (2001).
40. Q. Cui, M. Karplus, *Adv. Prot. Chem.* **66**, 315 (2003).
41. J. Villa, A. Warshel, *J. Phys. Chem. B* **105**, 7887 (2001).
42. A. R. Dinner, G. M. Blackburn, M. Karplus, *Nature* **413**, 752 (2001).
43. J. C. Fromme, S. D. Bruner, W. Yang, M. Karplus, G. L. Verdine, *Nature Struct. Biol.* **10**, 204 (2003).
44. I. Feierberg, J. Aqvist, *Theor. Chem. Acc.* **108**, 71 (2002).
45. Q. Cui, M. Karplus, *J. Am. Chem. Soc.* **123**, 2284 (2001).
46. Another enzyme in which a neutral histidine and electrostatic effects have been shown to be important is citrate synthase (*128*).
47. D. Joseph, G. A. Petsko, M. Karplus, *Science* **249**, 1425 (1990).
48. J. Ishijima, T. Nakai, S. Kawaguchi, K. Hirotsu, S. Kuramitsu, *J. Biol. Chem.* **275**, 18939 (2000).
49. T. M. Larsen, J. E. Wedeking, I. Rayment, G. H. Reed, *Biochemistry* **35**, 1692 (1996).
50. C. Alhambra, J. Gao, J. C. Corchado, J. Villa, D. G. Truhlar, *J. Am. Chem. Soc.* **121**, 2253 (1999).
51. H. Liu, Y. Zhang, W. Yang, *J. Am. Chem. Soc.* **122**, 6560 (2000).
52. T. Hansson, P. Nordlund, J. Aqvist, *J. Mol. Biol.* **265**, 118 (1997).
53. C. Alhambra, L. Wu, Z.-Y. Zhang, J. Gao, *J. Am. Chem. Soc.* **120**, 3858 (1998).
54. A. S. Mildvan, *Proteins* **29**, 401 (1997).
55. M. Zhang, R. L. Van Etten, C. V. Stauffacher, *Biochemistry* **33**, 11097 (1994).
56. M. Zhang, M. Zhou, R. L. Van Etten, C. V. Stauffacher, *Biochemistry* **36**, 15 (1997).
57. L. Ridder, A. J. Mulholland, I. M. C. M. Rietjens, J. Vervoort, *J. Am. Chem. Soc.* **122**, 8728 (2000).
58. L. Ridder, J. N. Harvey, I. M. C. M. Rietjens, J. Vervoort, A. J. Mulholland, *J. Phys. Chem. B* **107**, 2118 (2003).
59. L. Ridder, I. M. C. M. Rietjens, J. Vervoort, A. J. Mulholland, *J. Am. Chem. Soc.* **124**, 9926 (2002).
60. K. E. Ranaghan *et al.*, *Mol. Phys.* **101**, 2695 (2003).
61. P. D. Lyne, A. J. Mulholland, W. G. Richards, *J. Am. Chem. Soc.* **117**, 11345 (1995).
62. M. M. Davidson, I. R. Gould, I. H. Hillier, *J. Chem. Soc. Perkin Trans.* **2**, 525 (1996).
63. H. Guo, Q. Cui, W. N. Lipscomb, M. Karplus, *Proc. Natl. Acad. Sci. U.S.A.* **98**, 9032 (2001).
64. H. Guo, Q. Cui, W. N. Lipscomb, M. Karplus, *Angew. Chem. Int. Ed.* **42**, 1508 (2003)
65. S. Hur, T. C. Bruice, *Proc. Natl. Acad. Sci. U.S.A.* **100**, 12015 (2003); see also (*129*).
66. J. Chandrasekhar, S. F. Smith, W. L. Jorgensen, *J. Am. Chem. Soc.* **107**, 154 (1985).
67. A. Shurki, M. Strajbl, J. Villa, A. Warshel, *J. Am. Chem. Soc.* **124**, 4097 (2002).
68. K. H. Verschueren, F. Seljee, H. J. Rozeboom, K. H. Kalk, B. W. Dijkstra, *Nature* **363**, 693 (1993).
69. D. G. Truhlar *et al.*, *Acc. Chem. Res.* **35**, 341 (2002).
70. J. Gao, D. G. Truhlar, *Annu. Rev. Phys. Chem.* **53**, 467 (2002).
71. T. C. Bruice, *Acc. Chem. Res.* **35**, 86 (2002).
72. C. Alhambra *et al.*, *J. Phys. Chem. B* **105**, 11326 (2001).
73. T. D. Poulsen, M. Garcia-Viloca, J. Gao, D. G. Truhlar, *J. Phys. Chem. B* **107**, 9567 (2003).
74. A. Warshel, M. Strajbl, J. Villa, J. Florian, *Biochemistry* **39**, 14728 (2000).
75. N. Wu, Y. Mo, J. Gao, E. F. Pai, *Proc. Natl. Acad. Sci. U.S.A.* **97**, 2017 (2000).
76. B. G. Miller, R. Wolfenden, *Annu. Rev. Biochem.* **71**, 847 (2002).
77. J. Gao, *Curr. Opin. Struct. Biol.* **13**, 184 (2003).
78. F. Mancia, G. A. Smith, P. R. Evans, *Biochemistry* **38**, 7999 (1999).
79. J. M. Pratt, in *Handbook on Metalloproteins*, I. Bertini, A. Sigel, H. Sigel, Eds. (Dekker, New York, 2001), pp. 603–668.
80. A. Dybala-Defratyka, P. Paneth, *J. Inorg. Biochem.* **86**, 681 (2001).
81. M. R. Sawaya, J. Kraut, *Biochemistry* **36**, 586 (1997).
82. C. J. Falzone, P. E. Wright, S. J. Benkovic, *Biochemistry* **33**, 349 (1994).
83. M. J. Osborne *et al.*, *Biochemistry* **40**, 9846 (2001).
84. J. B. Watney, P. K. Agarwal, S. Hammes-Schiffer, *J. Am. Chem. Soc.* **125**, 3745 (2003).
85. C. E. Cameron, S. J. Benkovic, *Biochemistry* **36**, 15792 (1997).
86. P. K. Agarwal, S. R. Billeter, S. Hammes-Schiffer, *J. Phys. Chem. B* **106**, 3283 (2002).
87. P. K. Agarwal, S. R. Billeter, P. T. R. Rajagopalan, S. J. Benkovic, S. Hammes-Schiffer, *Proc. Natl. Acad. Sci. U.S.A.* **99**, 2794 (2002).
88. M. Garcia-Viloca, J. Gao, D. G. Truhlar, *Biochemistry* **42**, 13558 (2003).
89. J. L. Radkiewciz, C. L. Brooks III, *J. Am. Chem. Soc.* **122**, 225 (2000).
90. L. Li, P. E. Wright, S. J. Benkovic, C. J. Falzone, *Biochemistry* **31**, 7826 (1992).
91. M. Garcia-Viloca, C. Alhambra, D. G. Truhlar, J. Gao, *J. Am. Chem. Soc.* **124**, 7268 (2002).
92. M. Garcia-Viloca, C. Alhambra, D. G. Truhlar, J. Gao, *J. Comp. Chem.* **24**, 643 (2003).
93. M. Garcia-Viloca, T. D. Poulsen, D. G. Truhlar, J. Gao, unpublished data.
94. T. C. Bruice, F. C. Lightstone, *Acc. Chem. Res.* **32**, 127 (1999).
95. T. C. Bruice, S. J. Benkovic, *Biochemistry* **39**, 6267 (2000).
96. L. Young, C. B. Post, *Biochemistry* **35**, 15129 (1996).
97. Focusing on NACs has the practical advantage that their probability of occurring can sometimes be estimated by molecular dynamics simulations with a molecular mechanics force field and may not require a quantum mechanical calculation [but see (*63*, *130*)]. However, there is an inherent difficulty in attempting to draw conclusions from NACs in that there does not seem to be a way of uniquely determining the NAC (e.g., unlike the transition state, it is not a stationary point on the surface, nor does it satisfy a variational criterion). As mentioned in the description of chorismate mutase catalysis (*63*, *64*), an essential conformational change of the substrate is induced by the enzyme as a contribution to lowering the activation free energy. This shows that the phenomenon emphasized in the NAC concept can be very important in some cases. However, the conclusion in (*65*) that almost the entire barrier lowering is due to the conformational change is in disagreement with other analyses (*60*, *64*). For another example, Shurki *et al.* (*67*) designed

a simulation to evaluate the free energy effect of restricting the reactant conformational space for haloalkane dehalogenase and found a contribution of only 1 to 2 kcal/mol, relative to the full 7 kcal catalytic barrier lowering. The transition-state approach is general enough to include conformational effects when they are important, and it provides a unified framework that is also valid when conformational effects are negligible.

98. J. Hermans, L. Wang, *J. Am. Chem. Soc.* **119**, 2707 (1997).
99. B. Kuhn, P. A. Kollman, *J. Am. Chem. Soc.* **122**, 2586 (2000).
100. G. Careri, P. Fasella, E. Gratton, *Crit. Rev. Biochem.* **3**, 141 (1975).
101. G. R. Welch, B. Somogi, S. Damjanovich, *Prog. Biophys. Mol. Biol.* **39**, 109 (1982).
102. E. Neria, M. Karplus, *Chem. Phys. Lett.* **267**, 23 (1997).
103. K. Nam *et al.*, *J. Am. Chem. Soc.*, in press.
104. T. C. Allison, D. G. Truhlar, in *Modern Methods for Multidimensional Dynamics Computations in Chemistry*, D. L. Thompson, Ed. (World Scientific, Singapore, 1998), pp. 618–712.
105. C. Alhambra, M. L. Sanchez, J. C. Corchado, J. Gao, D. G. Truhlar, *Chem. Phys. Lett.* **355**, 388 (2002).
106. S. Hammes-Schiffer, *Biochemistry* **41**, 13335 (2002).
107. B. C. Garrett, D. G. Truhlar, *J. Phys. Chem.* **84**, 805 (1980).
108. Q. Cui, M. Karplus, *J. Am. Chem. Soc.* **124**, 3093 (2002).
109. S. R. Billeter, S. P. Webb, T. Iordanov, P. K. Agarwal, S. Hammes-Schiffer, *J. Chem. Phys.* **114**, 6925 (2001).
110. M. J. Sutcliffe, N. S. Scrutton, *Eur. J. Biochem.* **269**, 3096 (2002).
111. G. Tresadorn *et al.*, *Faraday Discuss.* **122**, 223 (2002).
112. T. Jonsson, M. H. Glickman, S. Sun, J. P. Klinman, *J. Am. Chem. Soc.* **118**, 10319 (1996).
113. J. Basran, M. J. Sutcliffe, N. S. Scrutton, *Biochemistry* **38**, 3218 (1999).
114. D. Sun, V. Davidson, *Prog. React. Kinet. Mech.* **27**, 209 (2002).
115. G. Tresadorn *et al.*, *Chem. Phys. Lett.* **358**, 489 (2002).
116. C. Alhambra, J. C. Corchado, M. L. Sanchez, J. Gao, D. G. Truhlar, *J. Am. Chem. Soc.* **122**, 8197 (2000).
117. Q. Cui, M. Elstner, M. Karplus, *J. Phys. Chem. B* **106**, 2721 (2002).
118. M. Karplus, J. A. McCammon, *Annu. Rev. Phys. Chem.* **53**, 263 (1983).
119. K. O. Alper, M. Singla, J. L. Stone, C. K. Bagdassarian, *Protein Sci.* **10**, 1319 (2001).
120. W. Forst, *Unimolecular Reactions* (Academic Press, New York, 1973).
121. J. Troe, in *Kinetics of Gas Reactions*, W. Jost, Ed., vol. 6B of *Physical Chemistry: An Advanced Treatise*, H. Eyring, D. Henderson, W. Jost, Eds. (Academic Press, New York, 1975), pp. 835–929.
122. J. Ashcroft, C. L. Xie, J. J. Jonas, *Chem. Phys.* **90**, 5386 (1989).
123. M. A. Wilson, D. Chandler, *Chem. Phys.* **149**, 11 (1990).
124. T. D. H. Bugg, *Nat. Prod. Report* **18**, 465 (2001).
125. S. J. Benkovic, S. Hammes-Schiffer, *Science* **301**, 1196 (2003).
126. H. A. Kramers, *Physica* **7**, 284 (1940).
127. R. M. Levy, M. Karplus, J. A. McCammon, *Chem. Phys. Lett.* **65**, 4 (1979).
128. A. J. Mulholland, W. G. Richards, *Proteins* **27**, 9 (1997)
129. Commentary by R. Schowen, *Proc. Natl. Acad. Sci. U.S.A.* **100**, 11931 (2003)
130. E. Y. Lau, K. Kahn, P. A. Bash, T. C. Bruice, *Proc. Natl. Acad. Sci. U.S.A.* **97**, 9937 (2000).
131. We thank A. S. Mildvan, G. A. Petsko, and R. L. Schowen for helpful comments on the manuscript. M.K. and D.G.T. thank A. Kuppermann for many discussions concerning reaction rate theory; the idea of doing this review first arose in a discussion at his 75th birthday symposium in which both of us participated. One of the authors (M.K.) thanks D. Case for illuminating discussions of reaction rate theory, which took place about 30 years ago. This work was supported in part by grants from the NSF and NIH. M.G.-V. thanks the Fulbright Commission and the Government of Catalonia for a scholarship.

Supporting Online Material

www.sciencemag.org/cgi/content/full/303/5655/186/DC1

Fig. S1

References